OPEN

Oncogene (2013), 1–12

www.nature.com/onc

ORIGINAL ARTICLE

The Polycomb group (PcG) protein EZH2 supports the survival of PAX3-FOXO1 alveolar rhabdomyosarcoma by repressing *FBXO32* (*Atrogin1/MAFbx*)

R Ciarapica[1,19], M De Salvo[1,19], E Carcarino[2,20], G Bracaglia[1,20], L Adesso[1], PP Leoncini[1], A Dall'Agnese[2], ZS Walters[3], F Verginelli[1], L De Sio[1], R Boldrini[4], A Inserra[5], G Bisogno[6], A Rosolen[6], R Alaggio[7], A Ferrari[8], P Collini[9], M Locatelli[10], S Stifani[11], I Screpanti[12], S Rutella[1], Q Yu[13], VE Marquez[14], J Shipley[3], S Valente[15], A Mai[15], L Miele[16], PL Puri[2,17], F Locatelli[1,18], D Palacios[2] and R Rota[1]

The Polycomb group (PcG) proteins regulate stem cell differentiation via the repression of gene transcription, and their deregulation has been widely implicated in cancer development. The PcG protein Enhancer of Zeste Homolog 2 (EZH2) works as a catalytic subunit of the Polycomb Repressive Complex 2 (PRC2) by methylating lysine 27 on histone H3 (H3K27me3), a hallmark of PRC2-mediated gene repression. In skeletal muscle progenitors, EZH2 prevents an unscheduled differentiation by repressing muscle-specific gene expression and is downregulated during the course of differentiation. In rhabdomyosarcoma (RMS), a pediatric soft-tissue sarcoma thought to arise from myogenic precursors, EZH2 is abnormally expressed and its downregulation *in vitro* leads to muscle-like differentiation of RMS cells of the embryonal variant. However, the role of EZH2 in the clinically aggressive subgroup of alveolar RMS, characterized by the expression of PAX3-FOXO1 oncoprotein, remains unknown. We show here that EZH2 depletion in these cells leads to programmed cell death. Transcriptional derepression of F-box protein 32 (*FBXO32*) (*Atrogin1/MAFbx*), a gene associated with muscle homeostasis, was evidenced in PAX3-FOXO1 RMS cells silenced for EZH2. This phenomenon was associated with reduced EZH2 occupancy and H3K27me3 levels at the *FBXO32* promoter. Simultaneous knockdown of FBXO32 and EZH2 in PAX3-FOXO1 RMS cells impaired the pro-apoptotic response, whereas the overexpression of FBXO32 facilitated programmed cell death in EZH2-depleted cells. Pharmacological inhibition of EZH2 by either 3-Deazaneplanocin A or a catalytic EZH2 inhibitor mirrored the phenotypic and molecular effects of EZH2 knockdown *in vitro* and prevented tumor growth *in vivo*. Collectively, these results indicate that EZH2 is a key factor in the proliferation and survival of PAX3-FOXO1 alveolar RMS cells working, at least in part, by repressing *FBXO32*. They also suggest that the reducing activity of EZH2 could represent a novel adjuvant strategy to eradicate high-risk PAX3-FOXO1 alveolar RMS.

Oncogene advance online publication, 11 November 2013; doi:10.1038/onc.2013.471

Keywords: EZH2; FBXO32; histone methyltransferases; PAX3-FOXO1; rhabdomyosarcoma; Polycomb proteins

INTRODUCTION

Rhabdomyosarcomas (RMS) are heterogeneous highly malignant tumors, which account for 7–8% of all pediatric malignancies and over half of the soft-tissue sarcomas in children. RMS are classically subdivided in two major histotypes: embryonal (around 70–80%) and alveolar (around 20–30%), the latter often metastatic at diagnosis and showing a high risk of recurrence.[1] In 70% of cases, alveolar RMS is characterized by the chromosomal translocation *t*(2;13) or *t*(1;13), resulting in PAX3-FOXO1 or PAX7/FOXO1 fusion oncoproteins that are considered the key negative prognostic molecular markers.[1,2] Current therapy regimens for high-risk RMS are often associated with significant morbidity in young patients and are often ineffective in preventing tumor progression. Although the expression of the muscle regulatory factor MyoD suggests their myogenic origin, the RMS cells fail to activate the differentiation program in response to physiological stimuli,[3] and we and others have shown that enforced induction of

[1]Department of Oncohematology, Ospedale Pediatrico Bambino Gesù, IRCCS, Roma, Italy; [2]IRCCS Fondazione Santa Lucia, Roma, Italy; [3]Sarcoma Molecular Pathology, Divisions of Molecular Pathology and Cancer Therapeutics, The Institute of Cancer Research, Sutton, UK; [4]Department of Pathology, Ospedale Pediatrico Bambino Gesù, IRCCS, Roma, Italy; [5]Department of Surgery, Ospedale Pediatrico Bambino Gesù, IRCCS, Roma, Italy; [6]Department of Pediatrics, Oncohematology Unit, University of Padova, Padova, Italy; [7]Medicine DIMED, Pathology Unit, University of Padova, Padova, Italy; [8]Pediatric Oncology Unit, Fondazione IRCCS Istituto Nazionale dei Tumori, Milano, Italy; [9]Anatomic Pathology Unit 2, Fondazione IRCCS Istituto Nazionale dei Tumori, Milano, Italy; [10]Scientific Directorate, Ospedale Pediatrico Bambino Gesù, IRCCS, Roma, Italy; [11]Centre for Neuronal Survival, Montreal Neurological Institute, McGill University, Montreal, Quebec, Canada; [12]Department of Molecular Medicine, Sapienza University, Roma, Italy; [13]Cancer Therapeutics and Stratified Oncology, Genome Institute of Singapore, Agency for Science, Technology and Research, Singapore; [14]Chemical Biology Laboratory, Frederick National Laboratory for Cancer Research, CCR, National Cancer Institute, NIH, Frederick, MD, USA; [15]Istituto Pasteur, Fondazione Cenci Bolognetti, Dipartimento di Chimica e Tecnologie del Farmaco, Sapienza University, Roma, Italy; [16]Cancer Institute, University of Mississippi Medical Center, Jackson, MS, USA; [17]Muscle Development and Regeneration Program, Sanford-Burnham Medical Research Institute, La Jolla, CA, USA and [18]Dipartimento di Scienze Pediatriche, Università di Pavia, Pavia, Italy. Correspondence: Dr R Rota, Department of Oncohematology, Laboratory of Angiogenesis, Ospedale Pediatrico Bambino Gesù, IRCCS, Piazza S. Onofrio 4, Roma 00165, RM, Italy or Dr D Palacios, IRCCS Fondazione Santa Lucia, Via del Fosso di Fiorano, 64, Roma 00143, Italy.
E-mail: rossella.rota@opbg.net or d.palacios@hsantalucia.it
[19]These authors contributed equally to this work.
[20]These authors contributed equally to this work.
Received 14 May 2013; revised 11 September 2013; accepted 30 September 2013

myogenic differentiation leads to the loss of malignant phenotype *in vitro* and *in vivo*.[3–6]

In vertebrates, Polycomb Group proteins form two main groups of multiprotein complexes, Polycomb Repressive Complex (PRC)-1 and PRC2.[7] The enhancer of Zeste Homolog 2 (EZH2), the catalytic subunit of PRC2, methylates lysine 27 of histone H3 (H3K27me3), a hallmark of PRC2-mediated gene repression.[8] EZH2 is down-regulated during progenitor cell differentiation, being undetectable in adult specialized cells and tissues.[8] Conversely, EZH2 is abnormally expressed in a wide range of tumors, with its level of expression being correlated with cancer aggressiveness.[8] In undifferentiated muscle cells, EZH2-mediated trimethylation of H3K27 contributes to maintaining the chromatin of muscle genes in a conformation repressive for transcription, supporting the self-renewal and proliferation of progenitor cells.[9–13] At the onset of differentiation, downregulation of EZH2 allows a chromatin conformation permissive for transcription of differentiation genes.[11–13] These data highlight the importance of EZH2 in controlling the balance between proliferation and differentiation of myogenic progenitors.

A number of reports have shown that aberrant overexpression of EZH2 in human cancers is often associated with poor prognosis.[14–18] EZH2 is expressed in undifferentiated stem-like cancer cells and promotes cancer cell proliferation and metastasis formation by repressing several tumor suppressor genes.[15,19–24] Notably, its molecular or pharmacological inhibition leads to the reversal of the malignant phenotype.[24–29] Collectively, these findings demonstrate a role of EZH2 as a potential prognostic marker and therapeutic target in cancer. We and others have recently reported that (i) as compared with the normal myoblasts and muscle tissues EZH2 is markedly overexpressed in RMS[30,31] and (ii) EZH2 downregulation *in vitro* leads to myogenic-like differentiation of an embryonal RMS cell line.[32]

However, the role of EZH2 in the aggressive PAX3-FOXO1 alveolar RMS cells has not been evaluated, and the effect of EZH2 inhibition on the tumorigenic phenotype remains to be tested.

In the present work, we sought to evaluate the response of alveolar RMS expressing the PAX3-FOXO1 oncoprotein to EZH2 inhibition and to dissect the underlying molecular mechanisms. We show that EZH2 depletion induced apoptosis of this subtype of RMS cells in part through the derepression of the EZH2 target gene F-box protein 32 (*FBXO32*), also known as *Atrogin1/MAFbx*. Consistently, FBXO32 depletion rescues, whereas its overexpression facilitates, the pro-apoptotic effect of EZH2 silencing.

Pharmacological inhibition of EZH2 using 3-Deazaneplanocin A (DZNep), an S-adenosyl-L-homocysteine hydrolase inhibitor that induces proteosome-mediated degradation of EZH2,[25] or MC1945, a catalytic EZH2 inhibitor,[33,34] phenocopies EZH2 knockdown effects *in vitro* and hampers tumor xenograft growth *in vivo*. Altogether, these results identify a key function of EZH2 in promoting the survival of PAX3-FOXO1 alveolar RMS that involves, at least partially, the modulation of *FBXO32* expression. They also indicate that affecting EZH2 activity either by depletion or by inactivation could provide an anticancer strategy in this high-risk subgroup of pediatric soft-tissue sarcomas.

RESULTS

EZH2 protein levels are elevated in human PAX3-FOXO1 RMS primary samples and cell lines

We first evaluated whether, as we recently reported for EZH2 transcripts,[30,31] EZH2 protein levels were higher in PAX3-FOXO1 RMS tumor samples than in normal muscle tissue. EZH2 was studied using immunohistochemical analysis on 10 primary samples from PAX3-FOXO1-bearing alveolar RMS patients (Supplementary Table 1). EZH2 nuclear staining was detected in all the RMS specimens tested with median values ranging from 46 to 92% of positive nuclei per section, whereas normal muscles were negative (Figure 1a).

In line with data on primary tumors, EZH2 levels were higher in PAX3-FOXO1-positive alveolar RMS cell lines compared with control skeletal myoblasts (skeletal muscle cells) and the protein was mostly localized in the nuclear-enriched fractions (Figure 1b). Moreover, unlike what typically observed in myoblasts during differentiation, EZH2 levels were not modulated when RMS cells were incubated in differentiation culture conditions (low serum-containing medium) (Figure 1c).[11] These findings imply that EZH2 expression and/or stability is deregulated in PAX3-FOXO1 alveolar RMS.

Downregulation of EZH2 prevents PAX3-FOXO1 RMS cell proliferation

As EZH2 expression sustains the proliferation of skeletal muscle precursors,[9–11] we sought to examine the effect of EZH2 depletion on the proliferation potential of the PAX3-FOXO1 alveolar cell line RH30 cultured in a proliferation (growth) medium. Cells were subjected to a double round (24 h) of RNA interference with a previous validated pool of siRNAs against EZH2 to warrant efficient and sustained silencing and analyzed starting from 24 h after the first siRNA transfection. Interestingly, EZH2-depleted RH30 cells were unable to proliferate showing $12 \pm 3.5\%$ survival 3 days after siRNA treatment (Figure 2a), as detected by trypan blue exclusion. EZH2 silencing was confirmed by western blot from 24 h onward (Figure 2b). Consistently, a global decrease in H3K27me3, but not in trimethylated Lys4 (H3K4me3), was detected at day 3 post-EZH2 siRNA transfection (Figure 2c). These results indicate that EZH2 has a role in the proliferation and survival of PAX3-FOXO1 alveolar RMS cells.

Knockdown of EZH2 promotes apoptosis of PAX3-FOXO1 alveolar RMS cells

EZH2 depletion in RH30 and RH4, another PAX3-FOXO1 alveolar RMS cell line, resulted in an increase of the percentage of cells in the subG1 cell-cycle phase compared with control siRNA cells (28 ± 3 and $26 \pm 2\%$, respectively) (Figure 3a). This was associated with a decrease of the percentage of cells in G1 and S phases (30 ± 6 and $11 \pm 3\%$, and 28 ± 8 and $10 \pm 2\%$, respectively) and an increase by 20 ± 3 and $18 \pm 5\%$ of cells in G2 phase, respectively (Figure 3a). Among the pro-apoptotic genes derepressed upon EZH2 knockdown, we annotated the ubiquitin ligase *FBXO32* (*Atrogin 1/MFAbx*) (Figures 3b and c), a tumor suppressor gene that is repressed by EZH2 in several tumor cell types.[23] In contrast, the expression of another known pro-apoptotic EZH2 target gene BIM and that of BAX were not upregulated 48 h after EZH2 silencing in both cell lines (Figures 3b and c). Further, a decrease in Myogenin, MyoD and BCL2 protein levels and the appearance of a PARP-1-cleaved band in EZH2 siRNA cells compared with untreated or control siRNA cells (Figure 3c) indicated that the differentiation program was inhibited in favor of programmed cell death. The same effect was obtained in RH30 cells transfected with an siRNA targeting the 5′-UTR of EZH2 mRNA already used in our lab[22] (Supplementary Figures 1a and b) or infected with a lentivirus expressing a short hairpin RNA against EZH2 (Supplementary Figures 1c and d). Altogether, these results rule out siRNA off-target effects.

Conversely to what was observed in PAX3-FOXO1 RMS cells, EZH2 siRNA-mediated depletion in skeletal muscle cells cultured in GM resulted in no modulation in *FBXO32* transcript levels 48 h post siRNA treatment and was associated to sustained Myogenin mRNA and protein induction 48 and 96 h after silencing, respectively, compared with control siRNA cells (Supplementary Figures 2a and b). These findings confirm that the downregulation of EZH2 in normal myoblasts determine the triggering of a differentiation program as already reported.[11,35,36]

Finally, biochemical rescue experiments using a retroviral vector expressing the murine EZH2 (not targeted by the used EZH2 siRNA) abolished the upregulation of *FBXO32* in EZH2-depleted

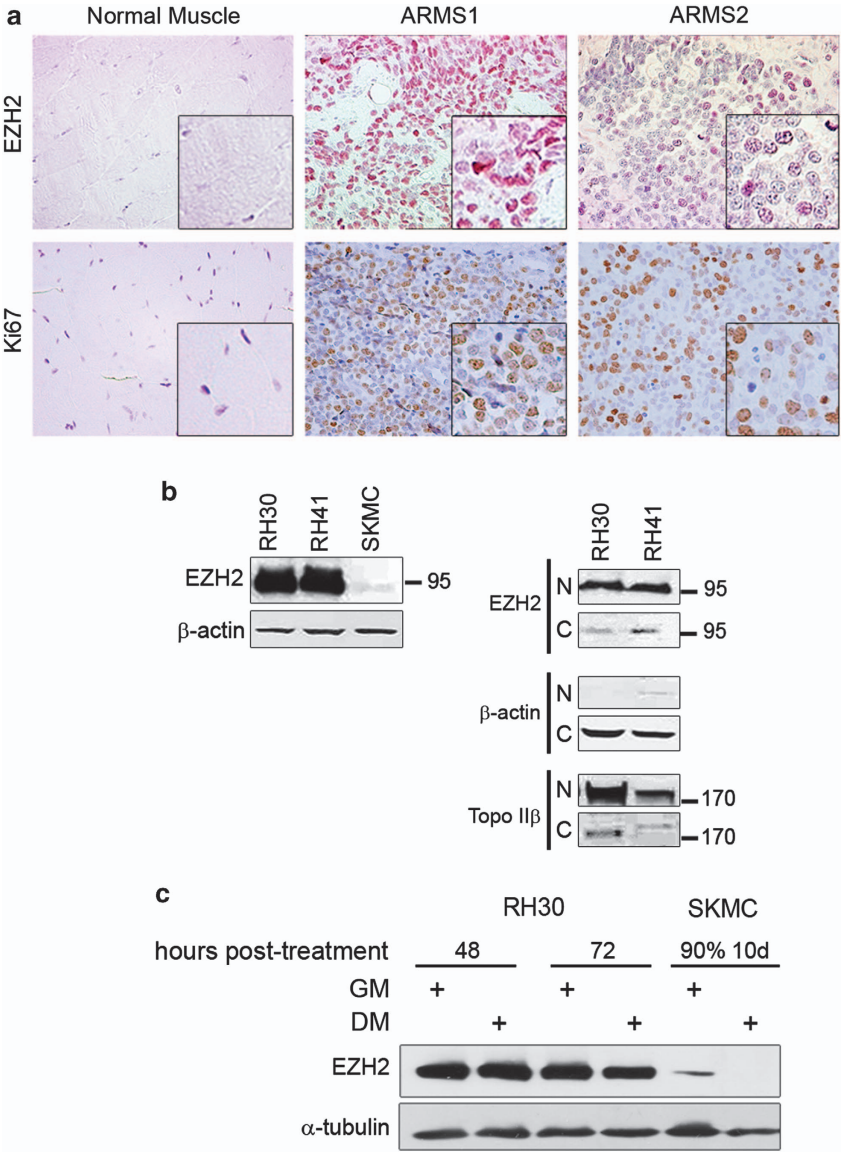

Figure 1. EZH2 protein levels are upregulated in primary PAX3-FOXO1 alveolar rhabdomyosarcoma (RMS) tissues and cell lines. (**a**) Representative immunohistochemical staining patterns showing EZH2 (upper panels) and Ki67 (bottom panels) expression in normal muscle and in primary tissue sections of alveolar PAX3-FOXO1 fusion-positive RMS specimens (ARMS). Brown-orange color in nuclei indicates positive staining (400X Magnification). Normal muscles are negative for both the markers. Insets represent a higher magnification of selected regions. (**b**, left) Western blot showing EZH2 and β-actin (loading control) in whole-cell lysates from PAX3-FOXO1 fusion-positive alveolar RMS cell lines and normal human myoblasts (SKMC) as control, all cultured in proliferating medium (that is, supplemented with 10% fetal calf serum). Representative of three independent experiments. (**b**, right) Western blot analysis of nuclear (N) and cytoplasmic (C)-enriched cell fractions of PAX3-FOXO1 alveolar RMS cell lines. Nuclear EZH2 was detected in the two cell lines. β-actin and topoisomerase IIβ were used as loading controls to discriminate the cytoplasmic and nuclear-enriched cell fractions, respectively. Representative of two independent experiments. (**c**) Western blot analysis showing EZH2 expression in PAX3-FOXO1 fusion-positive RH30 cells cultured for 48 and 72 h in either proliferating (growth) medium (GM) (that is, supplemented with 10% of fetal calf serum) or differentiating medium (DM) (that is, supplemented with 2% of horse serum). The last two lanes show EZH2 expression in SKMC cells cultured in either GM or DM medium. Ninety percent indicates the percentage of SKMC cell confluence in GM at which the cells were shifted to DM for 10 days (10d). α-tubulin was the loading control. Representative of two independent experiments.

RH30 cells (Supplementary Figure 3), indicating that the effect on *FBXO32* expression is mediated by EZH2.

Derepression of FBXO32 has a role in apoptosis induced by EZH2 depletion in PAX3-FOXO1 alveolar RMS cells

In agreement with cell cycle results and with data in Supplementary Figure 1, EZH2 siRNA transfection increased the percentage of Annexin V-positive (apoptotic) cells from 14 ± 3% in control siRNA to 46 ± 5% and from 14 ± 4 to 53 ± 7% in RH30 and RH4 cells, respectively (Figures 4a and b). Despite transfection with control siRNA showed a slight cytotoxic effect compared with the untransfected condition, the difference between control and EZH2 siRNA treatments was remarkable. Conversely, no Annexin V-positive cell population was detected after EZH2 knockdown in skeletal muscle cells cultured in GM (Supplementary Figure 2c) highlighting, once more, the different effects of this approach in a diverse cellular microenvironment. Notably, the percentage of Annexin V-positive cells decreased by 50% in EZH2-depleted RMS cells co-transfected with an FBXO32 siRNA. In contrast, enforced overexpression of

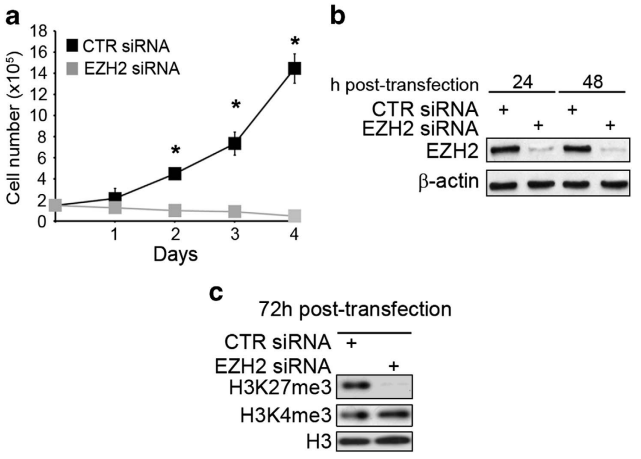

Figure 2. EZH2 depletion inhibits PAX3-FOXO1 fusion-positive alveolar rhabdomyosarcoma cell proliferation. (**a**) RH30 cells were transfected (Day 0) with EZH2 siRNA or control (CTR) siRNA and after 24 h transfected again (Day 1). Cells cultured in proliferating medium (that is, supplemented with 10% of fetal calf serum) were collected and counted starting from 24 h from the first siRNA transfection at the indicated time points. $*P < 0.05$ (Student's *t*-test); Bars, Standard Deviation (s.d.) of three replicates performed in duplicate. (**b**) Western blot showing levels of EZH2 24 and 48 h post transfection with CTR or EZH2 siRNA in RH30 cells. β-actin served as a loading control. Representative of four independent experiments. (**c**) Western blot showing histone H3 trimethylation status of Lys27 (H3K27me3) and Lys4 (H3K4me3) 72 h after EZH2 or CTR siRNA transfection. Histone H3 was the loading control. Representative of three replicates.

FBXO32 enhanced the apoptotic rate of about 40 and 65% in RH30 and RH4 cells after only 24 h of EZH2 knockdown (one round of silencing), respectively, while showed a slight effect in control siRNA cells (Figure 4c and Supplementary Figure 4). In agreement with what was observed after EZH2 silencing alone, this effect was associated with a decrease in MyoD and BCL2 (Figure 4d). Altogether, these data suggest that EZH2 supports the survival of PAX3-FOXO1 alveolar RMS cells at least in part by repressing *FBXO32*.

FBXO32 is directly targeted by EZH2 in PAX3-FOXO1 alveolar RMS cells

To confirm that *FBXO32* is a target gene of EZH2 in our cell context, we performed chromatin immunoprecipitation assays to evaluate the binding of EZH2 and the H3K27me3 status on the *FBXO32* promoter. Figure 5a shows that EZH2 recruitment decreased in EZH2-silenced RH30 cells as compared with control siRNA cells and this paralleled with a decrease in the levels of H3K27me3 at the Polycomb-dependent *FBXO32* promoter, pointing to *FBXO32* as a direct target of EZH2 in PAX3-FOXO1 alveolar RMS.

We previously reported that the Jumonji family member JARID2 cooperates with components of the PRC2 complex to regulate the H3K27me3 status on muscle regulatory genes in both embryonal and alveolar RMS cells. However, as shown in Supplementary Figure 5, JARID2 depletion by siRNA in PAX3-FOXO1 alveolar RMS cells did not affect H3K27me3 levels at the *FBXO32* promoter, as already reported in other cell contexts.[37,38]

Moreover, gene expression profiling data for 101 RMS previously described patient samples in the ITCC/CIT data set (Innovative Therapies for Children with Cancer/Carte d'Identité des Tumeurs)[1] within the R2 online platform[39] relative to publicly available Affymetrix expression profiling data for skeletal muscle samples (GSE9103), indicated that FBXO32 expression is much lower in RMS patient samples relative to skeletal muscle (Figure 5b), which is in direct contrast to EZH2 levels in RMS patient samples where EZH2 is overexpressed, as previously reported by our group.[30] Finally, the analysis of the RMS patient sample set also showed a significant negative correlation between FBXO32 and EZH2 expression in RMS patient samples ($R = -0.5$, $P = 1.0e-07$), once again indicating an inverse relationship between the levels of these two proteins that supports their functional interactions (Figure 5c).

Altogether, these results suggest that EZH2 directly regulates FBXO32 expression in PAX3-FOXO1 alveolar RMS cells and that it could also be involved in maintaining low expression levels *in vivo*.

Pharmacological inhibition of EZH2 prevents PAX3-FOXO1 RMS cell proliferation

As no direct catalytic EZH2 inhibitors were commercially available so far, we decided to pharmacologically inhibit EZH2 through two different approaches by treating cells with either (i) the S-adenosyl-L-homocysteine hydrolase inhibitor DZNep that indirectly inhibits EZH2 function mainly through degradation[23,24,40] or (ii) a catalytic EZH2 inhibitor, MC1945, the more recent synthesized compound from a family of EZH2 inhibitors validated against a panel of histone methyltransferases.[33,34] In preliminary experiments, MC1945 behaved similarly but at lower doses to the family-related EZH2 catalytic inhibitor MC1948 (Supplementary Figure 6) previously used by our group to inhibit EZH2 in myoblasts[41] and was therefore used in the subsequent assays. This experimental strategy was aimed at evaluating the ability of two different pharmacological types of inhibition to mimic the effects of siRNA-mediated depletion of EZH2 *in vitro*.

First, we characterized the effects of DZNep and MC1945 on the proliferation of PAX3-FOXO1-positive RMS cells and their capability to reduce H3K27marks. As shown in Figure 6a, 96 h treatment with 5 μM of either DZNep or MC1945 achieved a significant inhibition of cell proliferation compared with vehicle-treated or untreated cells, respectively. DZNep treatment resulted in the downregulation of EZH2 protein levels, whereas, in line with a role as a catalytic inhibitor, MC1945 treatment did not affect them. Importantly, both treatments resulted in a marked decrease in global levels of H3K27me3 (Figure 6b), as previously reported,[25,40,41] whereas the levels of H3K9me3, another repressive mark, remained unchanged demonstrating that they act mainly through inhibition of EZH2-containing complexes at the used doses on the basis of previous reports for DZNep.[24,40,42–45] Consistently with EZH2 silencing-dependent effects, the appearance of apoptotic Annexin V-positive cells was seen in both DZNep- and MC1945-treated RH30 cells (Figure 6c) associated with transcriptional upregulation of *FBXO32* gene and decreased Myogenin levels after 72 h (Figure 6d). Collectively, these observations indicate that pharmacological approaches either favoring the degradation or blocking the catalytic functions of EZH2 affect the proliferative potential of PAX3-FOXO1-positive alveolar RMS cells and mirror the effect of siRNA- and short hairpin RNA-mediated EZH2 depletion in derepressing *FBXO32*.

Pharmacological inhibition of EZH2 prevents PAX3-FOXO1 RMS tumor growth *in vivo*

We then evaluated whether inhibition of EZH2 functions through DZNep or MC1945 treatment could be a potential approach to treat PAX3-FOXO1 RMS also *in vivo*. Nude mice were inoculated with RH30 cells and, when tumors became palpable, intraperitoneally treated either with 2.5 mg/kg DZNep, a previously reported non-toxic dose in these conditions, or with a vehicle.[19,24] DZNep treatment resulted in a significant reduction in xenograft tumor volume (Figure 7a, left panels) and was associated with a decrease in the number of EZH2- and Ki67-positive cells (Figure 7b, upper panels). In agreement with *in vitro* results, a marked decrease in EZH2 protein levels was detected in DZNep-treated xenografts (Figure 7c). Similar results were obtained when mice were treated with 2.5 mg/kg of MC1945 (Figure 7a, right panels), which did not decrease EZH2 levels, as previously

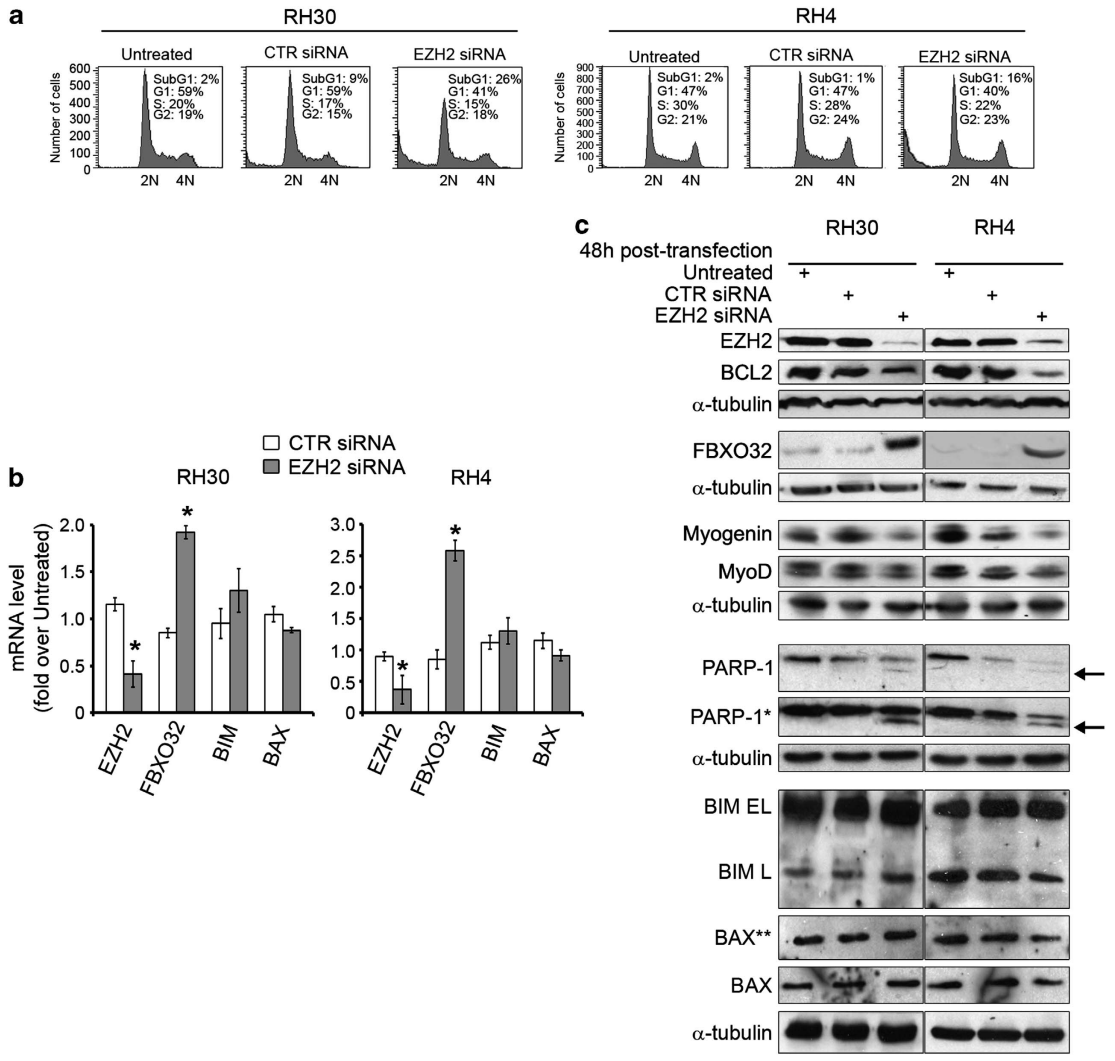

Figure 3. EZH2 depletion induces apoptosis of PAX3-FOXO1 alveolar RH30 and RH4 cells. (**a**) Cells were transfected (t0) with EZH2 siRNA or control (CTR) siRNA and after 24 h transfected again or left untransfected. Twenty-four hours after the second siRNA transfection, cells were collected for flow cytometry analysis. Twenty thousand events per sample were acquired. The histograms depict the percentage of Untreated, CTR or EZH2 siRNA-transfected RH30 (Left) and RH4 (Right) cells in the subG1, G1, S and G2 phases. Representative of three independent experiments performed in duplicate. (**b**) mRNA levels (real-time qRT-PCR) of EZH2, FBXO32, BIM and BAX in RH30 and RH4 cells 24 h after a double round of EZH2 siRNA treatment were normalized to GAPDH levels and expressed as a fold increase over Untreated condition (1 arbitrary unit, not reported). Columns, means; Bars, s.d. Results are the average of three independent experiments. *$P < 0.05$ (Student's *t*-test). (**c**) Western blot showing levels of EZH2, BCL2, FBXO32, Myogenin, MyoD, PARP-1 (black arrows indicate cleaved PARP-1), BIM, the activated form of BAX (BAX**), BAX and α-tubulin (loading control) in RH30 and RH4 cells 48 h after EZH2 or CTR siRNA transfection and in cells left untreated (Untreated). PARP-1* band: longer exposure. Representative of four independent experiments.

shown *in vitro* and confirmed here in xenografts using immunohistochemical analysis. An increase in TUNEL-positive cells was observed for both treatments consistent with the triggering of a pro-apoptotic program (Figure 7b, lower panels).

Collectively, our data provide evidence that EZH2 overexpression supports the survival of PAX3-FOXO1 alveolar RMS cells *in vivo* and suggest that targeting EZH2 might inspire novel therapeutic approaches to treat these high-risk alveolar RMS.

DISCUSSION

We have previously shown that EZH2 mRNA is overexpressed in cell lines and primary samples of pediatric RMS.[30,31] Moreover, EZH2 knockdown has been shown to induce *in vitro* differentiation of cells of the embryonal RMS subtype.[32] However, the effects of EZH2 downregulation in PAX3-FOXO1 alveolar RMS, clinically and molecularly distinct from the embryonal subtype[1,46–48] and considered as the highest-risk form of RMS,[2] remained unknown. The present work was aimed at evaluating whether the modulation of EZH2 could affect tumorigenesis and at dissecting the molecular events that underlie EZH2 function in this subgroup of RMS. We show here that, in addition, the EZH2 protein levels are significantly higher in PAX3-FOXO1 alveolar RMS primary tissues as compared with the normal muscle tissues. Moreover, unlike what happens in normal myoblasts,[11,35] the differentiation cue due to cell culture in the low-serum medium is unable to modulate the EZH2 levels in PAX3-FOXO1 alveolar RMS cells, indicating a tumor-specific deregulation.

We show here that EZH2 depletion highly affects PAX3-FOXO1 RMS cell survival leading to apoptosis. We then provide evidence that this phenomenon is due, at least in part, to the derepression of the tumor suppressor gene *FBXO32*, already shown to be induced by EZH2 knockdown in cells of solid and blood

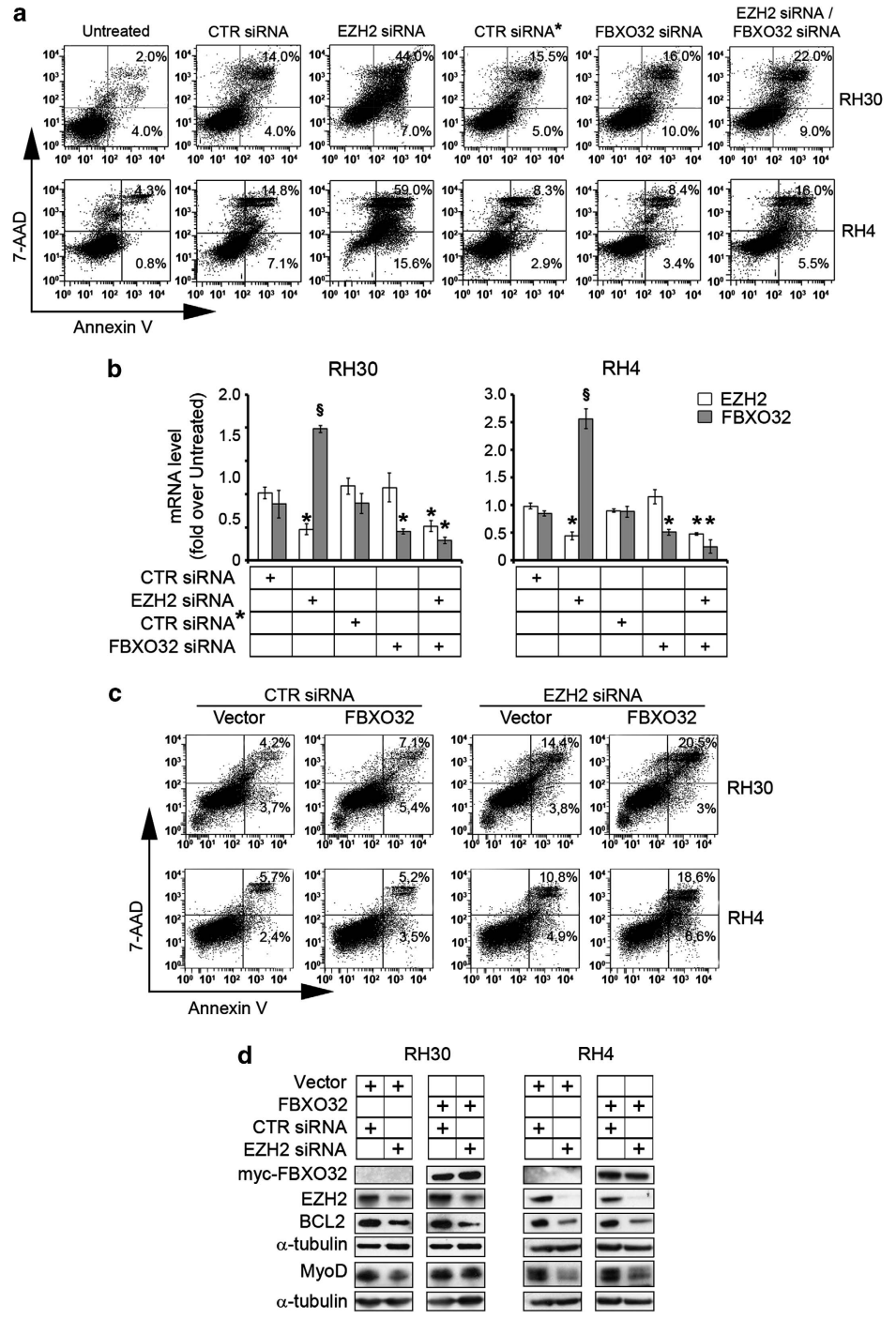

Figure 4. FBXO32 derepression is required for EZH2 knockdown-dependent apoptosis in PAX3-FOXO1 alveolar RMS cells. (**a**) RH30 and RH4 cells were transfected (double round) with either EZH2 siRNA or FBXO32 siRNA and with their control siRNAs (CTR siRNA and CTR siRNA*, respectively) or co-transfected with both EZH2 siRNA/FBXO32 siRNA or left untreated. Cells were stained for Annexin V and 7-AAD 24 h after the second round of silencing and the frequency of Annexin V and 7-AAD-positive labeling (% cell death) was recorded by flow cytometry. Samples were analyzed within 1 h. Representative cytofluorimetric plots are shown. Annexin V^+/7-AAD^- events (lower right quadrants) represent early stages of apoptosis, whereas Annexin V^+/7-AAD^+ events (upper right quadrants) stand for late apoptotic cells. Representative of three independent experiments run in duplicate. (**b**) mRNA levels (real-time qRT-PCR) of EZH2 and FBXO32 in RH30 and RH4 cells 24 h after the second round of siRNA transfection were normalized to GAPDH levels and expressed as a fold increase over the Untreated condition (1 arbitrary unit, not reported). Columns, means; Bars, s.d. Results are the average of three independent experiments. *$P<0.05$, §$P<0.01$ (Student's *t*-test). (**c**) RH30 and RH4 cells were infected (double round, see Methods) with either pMN-GFP control (Vector) or pMN-GFP myc-FBXO32 (FBXO32) overexpressing retroviral vectors. Twenty-four hours after the second infection, cells were transfected with either EZH2 siRNA or CTR siRNA, and 24 h after silencing cells were collected and analyzed for apoptosis. Cells were stained with Annexin V and 7-AAD, and the frequency of Annexin V and 7-AAD-positive labeling (% cell death) was recorded by flow cytometry. Representative cytofluorimetric plots are shown. Samples were analyzed within 1 h. Representative of three independent experiments run in duplicate. (**d**) Western blot from cells treated as in (**c**) showing levels of EZH2, BCL2, MyoD and α-tubulin (loading control) in RH30 and RH4 cells 24 h after the second round of silencing. Representative of two independent experiments.

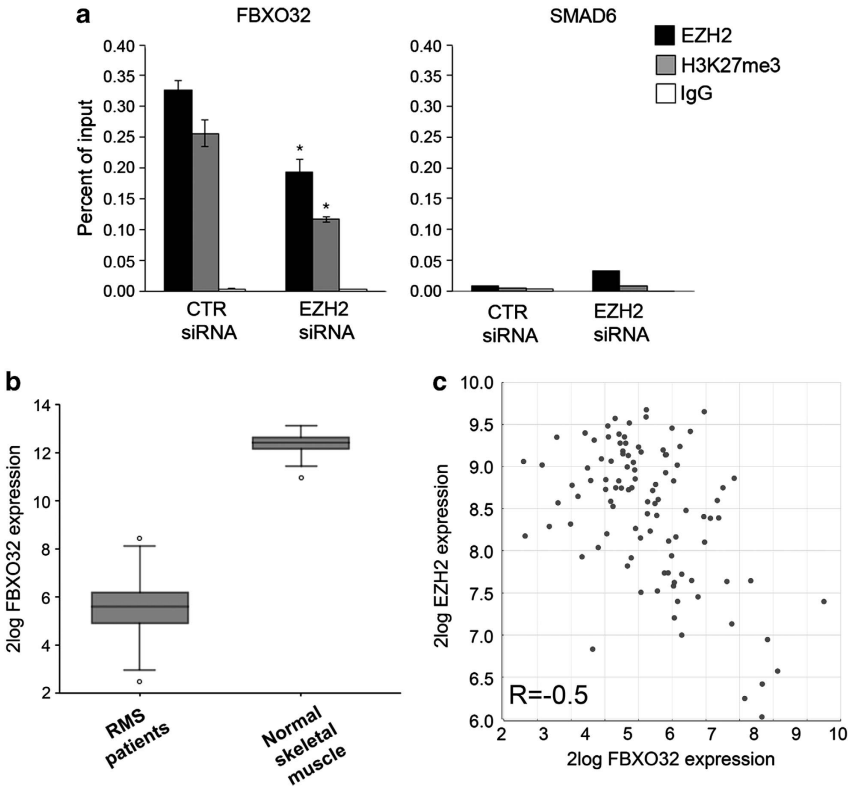

Figure 5. *FBXO32* is directly targeted by EZH2 and its expression is inversely correlated with EZH2 expression in RMS. (**a**) ChIP assays on RH30 cells 48 h after two rounds of EZH2 or CTR siRNA transfection showing the recruitment of EZH2 and the levels of histone H3 trimethylation on Lys27 (H3K27me3) on FBXO32 and a control gene (SMAD6) promoter. Normal rabbit IgG was used as a negative control. Graphs represent qPCR values normalized against input DNA. Results are the average of three independent experiments. $*P<0.05$ (Student's *t*-test). (**b**) *EZH2* expression levels from analyses of a previously published RMS patient ITCC/CIT data set (Innovative Therapies for Children with Cancer/Carte d'Identité des Tumeurs) within the R2 online platform ($R=-0.5$, $P=1.0e-07$) relative to skeletal muscle samples (GSE9103) using the R2 online platform. (**c**) Negative correlation between *EZH2* and *FBXO32* expression levels in the RMS patient set using the R2 online platform ($R=-0.5$, $P=1.0e-07$).

cancers.[23,28,40] Indeed, the simultaneous depletion of FBXO32 and EZH2 greatly reduced the apoptotic cell response, suggesting that EZH2 protects fusion-positive alveolar RMS cells from apoptosis in part by repressing *FBXO32*. Of note, *FBXO32* derepression is associated with both a reduction in EZH2 recruitment and a decrease in H3K27me3 mark to the *FBXO32* gene promoter, indicating that in our cell context EZH2 is recruited at this promoter and is enzymatically active to repress transcription, as already shown.[23,40] FBXO32, also known as Atrogin-1/MAFbx, is a muscle-specific E3 ligase involved in the massive protein degradation during muscle atrophy[49] and is a FOXO1 target gene in atrophic muscle.[50] However, there is no evidence for PAX3-FOXO1 directly regulating FBXO32 from analyses of ChIPseq data.[51] Recently, it has been shown that, in rat myoblasts *in vitro*, expression of FBXO32, which is induced in these cells by serum starvation, facilitates myogenesis through the repression of myocardin.[52] Intriguingly, both muscle atrophy and myogenesis involve apoptosis.[53–55] Moreover, the evidence that a same factor could have opposite effects on skeletal muscle, depending on the context, is not new and exemplified by Myogenin that can promote differentiation or degradation in different muscle microenvironments.[56] Therefore, the function of FBXO32 could be dependent from the molecular background and cellular normal or cancerous context.

Consistent with this idea, ectopic FBXO32 overexpression, although unable to induce *per se* consistent apoptosis, markedly enhances the cell death response in EZH2 knocked down cells, suggesting that it is required but insufficient to do so. It is, thus, conceivable that *FBXO32* expression may need to coordinate with other molecular events activating a global apoptotic program to sustain apoptosis in PAX3-FOXO1 RMS cells. This hypothesis is supported by the concomitant protein downregulation of Myogenin and MyoD seen in EZH2-depleted cells, the latter known as directly targeted by FBXO32 for degradation in myoblasts,[57–59] testifying the inability of our cells to undergo differentiation.[32] In addition, a decrease in BCL2, which has been shown to be degraded in cardiomyoblasts through a mechanism that indirectly involves FBXO32,[60] could support the triggering of an apoptotic process. These observations are in keeping with recently published data showing that the FBXO32 overexpression is not capable to induce apoptosis in the absence of chemotherapeutic drugs, although it is able to enhance the drug-induced pro-apoptotic effect in an 'activated' context.[23]

Interestingly, the modulation of JARID2, which can cooperate with components of the PRC2 at muscle-specific promoters in RMS, does not appear to affect H3K27me3 at the FBXO32 promoter suggesting that these two proteins do not cooperate to repress *FBXO32* expression in RMS cells, as reported for other target genes.[37,38] However, an EZH2-dependent regulation of FBXO32 expression in the RMS context is consistent with the observation that FBXO32 transcript levels are inversely correlated with those of EZH2 in patients and significantly reduced as compared with the levels in their normal counterparts. In contrast, EZH2 modulation has different effects in embryonal vs fusion-positive alveolar RMS cells. The embryonal cell subtype, indeed, as observed for myoblasts (refs 11,35,36 and our Supplementary Figure 2), undergo myogenic-like differentiation after both EZH2

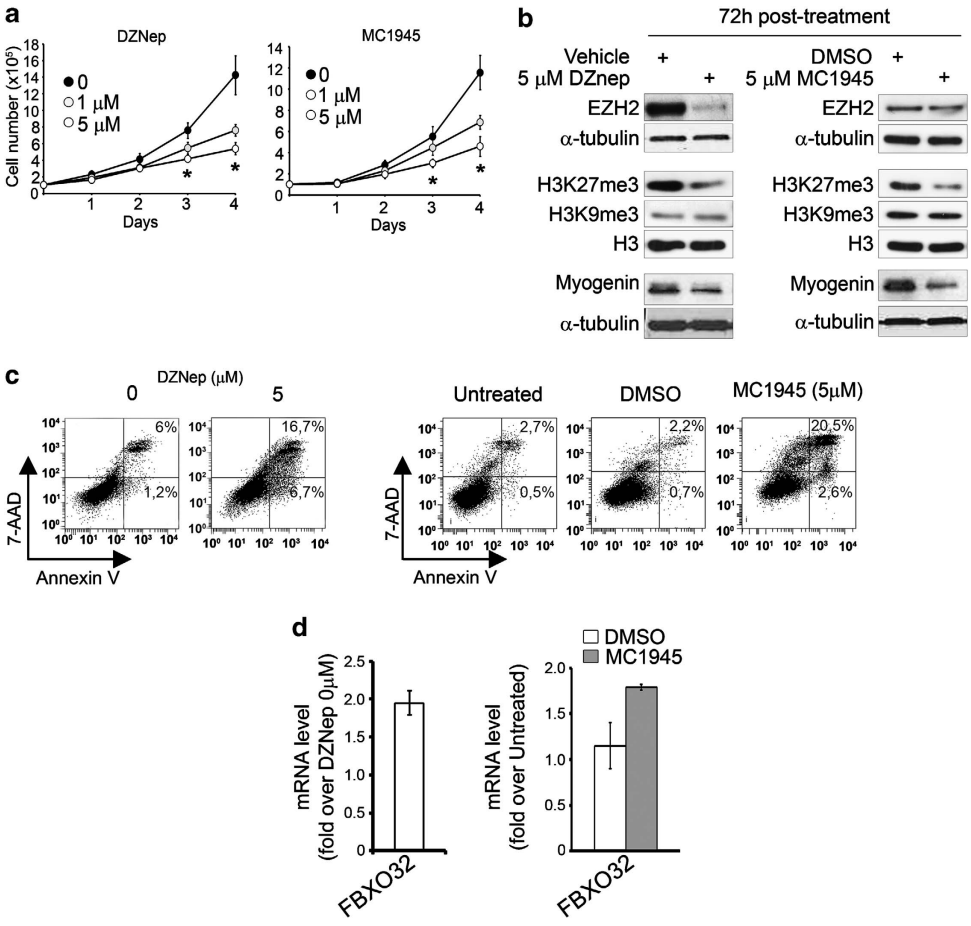

Figure 6. Pharmacological inhibition of EZH2 mimics the effects of EZH2 molecular silencing in PAX3-FOXO1 RMS cells. (**a**) RH30 cells cultured in proliferating medium (that is, supplemented with 10% of fetal calf serum) were treated daily with either the S-adenosyl-L-homocysteine hydrolase inhibitor 3-deazaneplanocin A (DZNep) (left panels) or the EZH2 catalytic inhibitor MC1945 (right panels) at the reported concentrations or with vehicle (that is, water for DZNep or DMSO for MC1945) and collected and counted at the indicated time points. *$P<0.05$ (Student's *t*-test); Bars, s.d. Results represent the average of three independent experiments performed in duplicate. (**b**) Western blot showing EZH2 levels along with histone H3 trimethylation on Lys27 (H3K27me3) and histone H3 trimethylation on Lys9 (H3K9me3) and Myogenin levels in RH30 cells treated for 72 h with 5 μM DZNep (left panel) and 5μM MC1945 (right panel) or with vehicle (that is, water or DMSO). Total H3 and α-tubulin were the loading controls. Representative of three independent experiments. (**c**) RH30 cells treated for 96 h with 5 μM DZNep (Left panels) or 5 μM MC1945 (Right panels) or with vehicle (that is, water or DMSO) or left untreated were stained for Annexin V and 7-AAD, and the frequency of Annexin V and 7-AAD-positive labeling (% cell death) was recorded by flow cytometry. Samples were analyzed within 1 h. Representative cytofluorimetric plots are shown. Annexin $V^+/7\text{-}AAD^-$ events (lower right quadrants) represent early stages of apoptosis, whereas Annexin $V^+/7\text{-}AAD^+$ events (upper right quadrants) stand for late apoptotic cells. Representative of three independent experiments run in duplicate. (**d**) mRNA levels (real-time qRT-PCR) of FBXO32 in RH30 cells treated for 72 h with 5 μM DZNep (Left) and 5 μM MC1954 (Right) or with vehicle (that is, water or DMSO) were normalized to GAPDH levels and expressed as a fold increase over Untreated condition (1 arbitrary unit, not reported). Columns, means; Bars, s.d. Results are the average of three independent experiments.

genetic silencing[32] and pharmacological inhibition (unpublished observations from our group). Differences in the response to the same treatment of RMS variants are not unusual and are in agreement with both the different cytogenetic and molecular background of fusion-positive alveolar RMS also related to the expression of PAX-FOXO1 chimeric proteins.[1,2,61–65]

Collectively, our data suggest that in PAX3-FOXO1 alveolar RMS EZH2 supports tumor cell survival at least in part by repressing *FBXO32*.

Very recently, some highly specific EZH2 inhibitors have been discovered and published.[26,27,29] In the attempt to evaluate the effect of pharmacologic inhibition of EZH2, we have used DZNep, which has been already shown to induce FBXO32 expression in cancer cells[25,28,40,66] in parallel with an EZH2 catalytic inhibitor, MC1945.[33,34] Both pharmacological treatments phenocopied the effects of genetic inhibition of EZH2 *in vitro* enhancing the apoptotic rate of fusion-positive alveolar RMS cells, upregulating *FBXO32* and downregulating Myogenin. Moreover, even if higher concentrations of DZNep compared with those used in this study can affect histone methyltransferases other than EZH2,[28] the decrease in H3K27me3, but not in H3K9me3 (another repressive transcriptional mark), observed after treatment with the two compounds suggests a selective function anti-EZH2.

Relevant under a translational point of view, *in vivo* studies showed that tumor growth is clearly impaired in animals in which the EZH2 function was blocked through the use of two different types of inhibitors, both leading to tumor cell apoptosis. These results suggest that EZH2 downregulation and/or inactivation could have an antitumor effect on PAX3-FOXO1-positive alveolar RMS *in vivo* being helpful in eradicating cancer cells, also in synergy with conventional chemotherapeutic compounds.

Growing evidence supports the use of epigenetic therapies in adult cancer patients.[67] In addition, in pediatric tumors of different origin, histone methyltransferase could become targets for novel

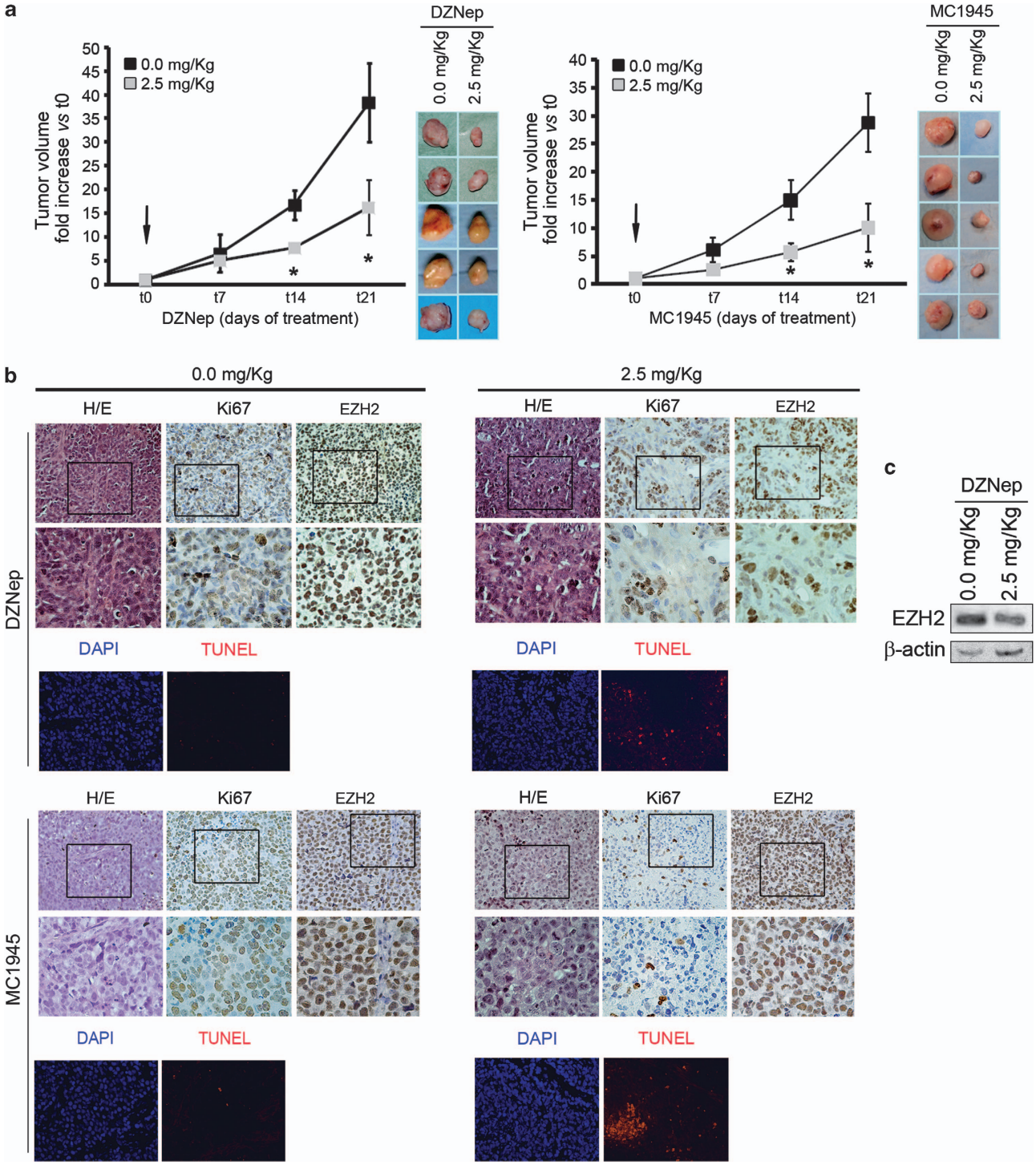

Figure 7. Pharmacological inhibition of EZH2 reduces alveolar RMS tumor growth *in vivo*. (**a**) Nude mice were inoculated with RH30 cell suspensions and when tumor became palpable (black arrow) animals were treated with or without 2.5 mg/kg of DZNep (left) and MC1945 (right) twice a day, 3 days per week for 3 weeks. The tumor volume was monitored weekly for 21 days after which xenografts were surgically removed (shown on the right of each graph). The mean of tumor volumes ($n = 5$ mice/group) was calculated and plotted against time in days using the s.d. (*$P < 0.05$, Kruskal – Wallis test). (**b**) Representative hematoxylin/eosin (H/E) staining and immunostaining patterns for Ki67 and EZH2 and TUNEL (apoptosis) staining of serial sections from xenografts excised at the end of DZNep treatment (upper panels) or MC1945 (bottom panels) (day 21). Nuclear brown-orange color indicates positive immune-stained cells and red fluorescence-positive apoptotic nuclei. For each H/E, Ki67 and EZH2 subgroup, 200X magnification (upper panels) and × 400 magnification (bottom panels) of selected regions are shown. (**c**) The expression of EZH2 was analyzed by western blot in lysates of pooled samples from DZNep-treated or untreated animals killed at day 21 (3 mice per group). β-actin was the loading control.

pharmacological therapies.[68] In summary, the data presented here provide evidence that the overexpression of EZH2 has a fundamental role in supporting the malignant potential of PAX3-FOXO1 alveolar RMS cells and that its depletion and/or inactivation could provide a potential effective strategy to treat these pediatric high-risk RMS.

MATERIALS AND METHODS

Cell lines

Human PAX3-FOXO1 RMS cell lines RH30 and RH41 were described previously,[6] and RH4 was a gift of C Ponzetto. Normal Human Skeletal Muscle cells (myoblasts) were obtained from PromoCell (Heidelberg, Germany). Supplementary methods describe cell lines and culture in detail.

Nuclear fraction enrichment

Cells were lysed and assayed as previously reported.[6]

Western blotting

Western blotting was performed on whole-cell lysates as previously described[6] with antibodies described in Supplementary Methods.

Histone extraction

Cells were collected and washed twice with ice-cold phosphate-buffered saline (PBS) 1X supplemented with 5 mM sodium butyrate. After resuspension in triton extraction buffer (PBS, 0.5% triton X 100 (v/v)) containing 2 mM PMSF and 0.02% (w/v) NaN3 at a cell density of 10^7 cells/ml, cells were lysated on ice for 10 min. Lysates were centrifuged at 2000 r.p.m. for 10 min at 4 °C, and the pellets were washed in half volume of triton extraction buffer and centrifuged as before. Pellets were then resuspended in 0.2 N HCl at a cell density of 4×10^7 cells/ml and histones were extracted O/N at 4 °C. Samples were then centrifuged and supernatants were used for western blot analysis.

Transient RNA interference

Cells were sequentially transfected or co-transfected by two subsequent rounds (24 h) (100 nM final concentration each round), unless otherwise stated, using Oligofectamine (Invitrogen, Carlsbad, CA, USA), according to the manufacturer's recommendations. ON-TARGET*plus* SMART pool siRNA against EZH2 (L-004218-00) or non-targeting siRNA (control; D-001206-13)[15,69,70] (Dharmacon, Thermo Fisher Scientific, Lafayette, CO, USA) or siRNA against FBXO32 (either Hs02_00362139 or EHU155831 MISSION esiRNA, Sigma, St Louis, MO, USA) or non-targeting siRNA controls (Sigma) were used.

Real-time qRT-PCR

Total RNA was extracted using TRizol according to the manufacturer's instructions (Invitrogen), and qRT-PCR was performed as described.[6] Taqman gene assays for GAPDH, EZH2, Myogenin and MCK were from Applied Biosystems (Life Technologies, Carlsbad, CA, USA) (Hs99999905_m1, Hs01072232_m1, Hs00176490_m1). Murine Ezh2, FBXO32, BIM and BAX mRNAs were quantified through the SYBR-green method (Applied Biosystems) with primers previously reported[23] or available on request.

Retroviral infections

The PMN-GFP retroviral vector expressing cMyc-tagged FBXO32 or control PMN-GFP empty vector was previously reported.[23] The pMSCV-GFP retroviral vector (Addgene, Cambridge, MA, USA) expressing flag-tagged murine EZH2 or control pMSCV-GFP empty vector was from G Caretti. Phoenix ampho cells obtained from ATCC were cultured in DMEM supplemented with 10% FBS and transiently transfected using lipofectamine (Invitrogen, Life Technologies). Supernatant containing viral particles collected after 48 h was used to infect RMS cells O/N in the presence of 5 μg/ml of polybrene (two rounds of infection).

Cell proliferation, cell cycle and apoptosis assays

For proliferation, cells were collected and counted at the reported time points. For cell cycle analysis, cells were collected 24 h after the second round of silencing and treated as previously reported.[6] For quantification of apoptosis, cells were stained in calcium-binding buffer with APC-conjugated Annexin V and 7-Aminoactinomycin D (7-AAD) using the Annexin V apoptosis detection kit (BD Pharmingen, San Diego, CA, USA), according to the manufacturer's recommendations. Cells were analyzed by a fluorescence-activated cell sorting using a FACSCantoII equipped with FACSDiva 6.1 CellQuest software (Becton Dickinson Instrument, San Jose, CA, USA).

Gene expression analysis

Affymetrix U133A plus 2.0 profiling data from 101 previously described patient samples[1] were analyzed using the R2 platform (Reference) using the 225328_at probe to detect FBXO32 and the 203358_s_at probe to detect EZH2 mRNA levels. The GSE9103 normal skeletal muscle data set within R2 was used for comparisons of FBXO32 levels between skeletal muscle and RMS patient samples.

Chromatin immunoprecipitation

The chromatin immunoprecipitation assay was performed as previously described.[71] The following antibodies were used: anti-H3K27me3 (EMD Millipore Corporation, Billerica, MA, USA) and anti-EZH2 (Diagenode s.a. Liège, Belgium). Real-time PCR was performed on input samples and equivalent amounts of immunoprecipitated material with the SYBR Green Master Mix (Applied Biosystems) with primers spanning FBXO32[23] and SMAD6 promoter regions as specified in the text (primer sequences available on request).

EZH2 inhibitory assay

The inhibitory assay for MC1945 against EZH2 has been already reported.[34]

Xenograft experiments and immunohistochemistry

Athymic 6-week-old female BALB/c nude mice ($nu^+\backslash nu^+$) were purchased from Charles River Laboratories (Calco (Lecco), Italy). Procedures involving animals were conformed to the institutional guidelines that comply with the national and international laws and policies (EEC Council Directive 86\609, OJ L 358, 12 December 1987). Animals were inoculated subcutaneously into the posterior flanks with RH30 cell suspensions in PBS (5×10^6 cells) and, when the tumors became palpable, intraperitoneally injected (5 mice/group) either with DZNep (2.5 mg/kg) or normal saline (vehicle) or with MC1945 (2.5 mg/kg) or DMSO (vehicle) twice daily, 3 days per week for 3 weeks when mice were killed with no visible signs of toxicity.[34,72] Tumor volume was measured as reported.[6] Sections from paraffin-embedded excised xenografts were stained with hematoxylin/eosin or immunohistochemically stained for EZH2 and Ki67 expression with antibodies and detection/acquisition methods reported below.

Immunohistochemistry on RMS primary tissues

Archival, de-identified formalin-fixed, paraffin-embedded PAX3-FOXO1 primary RMS and skeletal muscle control tissues were obtained from the Ospedale Pediatrico Bambino Gesù in Roma, University of Padova and Istituto Tumori di Milano, (Italy) after approval of the respective Institutional Review Boards. Clinicopathological characteristics of the cohort are reported in Supplementary Table 1. Histopathological features of the tumors were reviewed by a Pathologist of each Institution (RB, RA and PC) blinded to immunohistochemical results. Sections from RMS samples and four muscle tissue specimens were immunostained for EZH2 (Transduction Laboratories, BD, Franklin Lakes, NJ, USA)[73] and Ki67 (Novocastra, Newcastle upon Tyne, UK), and EnVision System-HRP (Power vision Plus method, Zymed, San Francisco, CA, USA) or Biotinilated link (DAKO, Carpintera, CA, USA) secondary antibodies were used followed by staining with 3-amino-9-ethylcarbazolo or 3,3′-diaminobenzidine (chromogen kits, DAKO) and counterstaining with Gill's hematoxylin (Bio-Optica, Milan, Italy). Negative controls were simultaneously stained either with isotype non-specific IgG or omitting the primary antibody. Each section was observed using an Eclipse E600 microscope (Nikon, Sesto Fiorentino, Firenze, Italy) and images were acquired through LUCIA software, version 4.81 (Nikon, Sesto Fiorentino, Firenze, Italy) with a Nikon Digital Camera DXM1200F.

Statistical analysis

The Student's *t*-test was performed to assess the difference between various treatments. $P<0.05$ was defined as the statistic significance. Continuous variables were analyzed by the Mann – Whitney *U*-test or the Kruskal – Wallis test for pairwise or multiple comparisons, respectively. Statistical significance was set at a two-tailed *P*-value <0.05. All analyses were performed with SPSS 11.5.1 for Windows Package (SPSS, Inc., 1989 – 2002 and LEADTOOLS 1991 – 2000, LEAD Technologies, Inc, Chicago, IL, USA).

CONFLICT OF INTEREST

The authors declare no conflict of interest.

ACKNOWLEDGEMENTS

We thank E Giorda for fluorescence-activated cell sorting analysis. Myogenin (Wright WE) and MHC (Fishman DA) antibodies were obtained from the Developmental Studies Hybridoma Bank, developed under the auspices of the NICHD and maintained by The University of Iowa, Department of Biology, Iowa City, IA 52242, USA. This work was supported by grants from Associazione Italiana per la Ricerca sul Cancro (AIRC, 10338) and Italian Ministry of Health Ricerca Corrente (RR); Association for International Cancer Research (AICR-UK, 12-0168) (DP); AIRC 5 per mille (FL); NIH Intramural Research Program, National Cancer Institute, CCR (VEM); Cancer Research UK (C5066/A10399) (ZSW); Sarcoma UK (ZSW, JS); Progetto IIT-Sapienza A2, FIRB RBFR10ZJQT and FP7 Project BLUEPRINT/282510 (AM). SS is a Chercheur National of the Fonds de la Recherche en Santé du Quebec.

REFERENCES

1 Williamson D, Missiaglia E, de Reynies A, Pierron G, Thuille B, Palenzuela G *et al.* Fusion gene-negative alveolar rhabdomyosarcoma is clinically and molecularly indistinguishable from embryonal rhabdomyosarcoma. *J Clin Oncol* 2010; **28**: 2151–2158.
2 Missiaglia E, Williamson D, Chisholm J, Wirapati P, Pierron G, Petel F *et al.* PAX3/FOXO1 fusion gene status is the key prognostic molecular marker in rhabdomyosarcoma and significantly improves current risk stratification. *J Clin Oncol* 2012; **30**: 1670–1677.
3 Puri PL, Wu Z, Zhang P, Wood LD, Bhakta KS, Han J *et al.* Induction of terminal differentiation by constitutive activation of p38 MAP kinase in human rhabdomyosarcoma cells. *Genes Dev* 2000; **14**: 574–584.
4 Wang H, Garzon R, Sun H, Ladner KJ, Singh R, Dahlman J *et al.* NF-kappaB-YY1-miR-29 regulatory circuitry in skeletal myogenesis and rhabdomyosarcoma. *Cancer Cell* 2008; **14**: 369–381.
5 Taulli R, Bersani F, Foglizzo V, Linari A, Vigna E, Ladanyi M *et al.* The muscle-specific microRNA miR-206 blocks human rhabdomyosarcoma growth in xenotransplanted mice by promoting myogenic differentiation. *J Clin Invest* 2009; **119**: 2366–2378.
6 Raimondi L, Ciarapica R, De Salvo M, Verginelli F, Gueguen M, Martini C *et al.* Inhibition of Notch3 signalling induces rhabdomyosarcoma cell differentiation promoting p38 phosphorylation and p21(Cip1) expression and hampers tumour cell growth in vitro and in vivo. *Cell Death Differ* 2012; **19**: 871–881.
7 Lanzuolo C, Orlando V. Memories from the polycomb group proteins. *Annu Rev Genet* 2012; **46**: 561–589.
8 Margueron R, Reinberg D. The Polycomb complex PRC2 and its mark in life. *Nature* 2011; **469**: 343–349.
9 Woodhouse S, Pugazhendhi D, Brien P, Pell JM. Ezh2 maintains a key phase of muscle satellite cell expansion but does not regulate terminal differentiation. *J Cell Sci* 2012; **126**: 565–579.
10 Juan AH, Derfoul A, Feng X, Ryall JG, Dell'Orso S, Pasut A *et al.* Polycomb EZH2 controls self-renewal and safeguards the transcriptional identity of skeletal muscle stem cells. *Genes Dev* 2011; **25**: 789–794.
11 Caretti G, Di Padova M, Micales B, Lyons GE, Sartorelli V. The Polycomb Ezh2 methyltransferase regulates muscle gene expression and skeletal muscle differentiation. *Genes Dev* 2004; **18**: 2627–2638.
12 Serra C, Palacios D, Mozzetta C, Forcales SV, Morantte I, Ripani M *et al.* Functional interdependence at the chromatin level between the MKK6/p38 and IGF1/PI3K/AKT pathways during muscle differentiation. *Mol Cell* 2007; **28**: 200–213.
13 Mousavi K, Zare H, Wang AH, Sartorelli V. Polycomb protein Ezh1 promotes RNA polymerase II elongation. *Mol Cell* 2012; **45**: 255–262.
14 Varambally S, Dhanasekaran SM, Zhou M, Barrette TR, Kumar-Sinha C, Sanda MG *et al.* The polycomb group protein EZH2 is involved in progression of prostate cancer. *Nature* 2002; **419**: 624–629.
15 Bracken AP, Pasini D, Capra M, Prosperini E, Colli E, Helin K. EZH2 is downstream of the pRB-E2F pathway, essential for proliferation and amplified in cancer. *Embo J* 2003; **22**: 5323–5335.
16 Raaphorst FM, Meijer CJ, Fieret E, Blokzijl T, Mommers E, Buerger H *et al.* Poorly differentiated breast carcinoma is associated with increased expression of the human polycomb group EZH2 gene. *Neoplasia* 2003; **5**: 481–488.
17 Kalushkova A, Fryknas M, Lemaire M, Fristedt C, Agarwal P, Eriksson M *et al.* Polycomb target genes are silenced in multiple myeloma. *PLoS One* 2010; **5**: e11483.
18 Rao ZY, Cai MY, Yang GF, He LR, Mai SJ, Hua WF *et al.* EZH2 supports ovarian carcinoma cell invasion and/or metastasis via regulation of TGF-beta1 and is a predictor of outcome in ovarian carcinoma patients. *Carcinogenesis* 2010; **31**: 1576–1583.
19 Kemp CD, Rao M, Xi S, Inchauste S, Mani H, Fetsch P *et al.* Polycomb repressor complex-2 is a novel target for mesothelioma therapy. *Clin Cancer Res* 2011; **18**: 77–90.
20 Yu J, Yu J, Rhodes DR, Tomlins SA, Cao X, Chen G *et al.* A polycomb repression signature in metastatic prostate cancer predicts cancer outcome. *Cancer Res* 2007; **67**: 10657–10663.
21 Suva ML, Riggi N, Janiszewska M, Radovanovic I, Provero P, Stehle JC *et al.* EZH2 is essential for glioblastoma cancer stem cell maintenance. *Cancer Res* 2009; **69**: 9211–9218.
22 Wu ZL, Zheng SS, Li ZM, Qiao YY, Aau MY, Yu Q. Polycomb protein EZH2 regulates E2F1-dependent apoptosis through epigenetically modulating Bim expression. *Cell Death Differ* 2010; **17**: 801–810.
23 Wu Z, Lee ST, Qiao Y, Li Z, Lee PL, Lee YJ *et al.* Polycomb protein EZH2 regulates cancer cell fate decision in response to DNA damage. *Cell Death Differ* 2011; **18**: 1771–1779.
24 Wang C, Liu Z, Woo CW, Li Z, Wang L, Wei JS *et al.* EZH2 Mediates epigenetic silencing of neuroblastoma suppressor genes CASZ1, CLU, RUNX3, and NGFR. *Cancer Res* 2011; **72**: 315–324.
25 Fiskus W, Wang Y, Sreekumar A, Buckley KM, Shi H, Jillella A *et al.* Combined epigenetic therapy with the histone methyltransferase EZH2 inhibitor 3-deazaneplanocin A and the histone deacetylase inhibitor panobinostat against human AML cells. *Blood* 2009; **114**: 2733–2743.
26 Qi W, Chan H, Teng L, Li L, Chuai S, Zhang R *et al.* Selective inhibition of Ezh2 by a small molecule inhibitor blocks tumor cells proliferation. *Proc Natl Acad Sci USA* 2012; **109**: 21360–21365.
27 Knutson SK, Wigle TJ, Warholic NM, Sneeringer CJ, Allain CJ, Klaus CR *et al.* A selective inhibitor of EZH2 blocks H3K27 methylation and kills mutant lymphoma cells. *Nat Chem Biol* 2012; **8**: 890–896.
28 Fiskus W, Rao R, Balusu R, Ganguly S, Tao J, Sotomayor E *et al.* Superior efficacy of a combined epigenetic therapy against human mantle cell lymphoma cells. *Clin Cancer Res* 2012; **18**: 6227–6238.
29 McCabe MT, Ott HM, Ganji G, Korenchuk S, Thompson C, Van Aller GS *et al.* EZH2 inhibition as a therapeutic strategy for lymphoma with EZH2-activating mutations. *Nature* 2012; **492**: 108–112.
30 Walters ZS, Villarejo-Balcells B, Olmos D, Buist TW, Missiaglia E, Allen R *et al.* JARID2 is a direct target of the PAX3-FOXO1 fusion protein and inhibits myogenic differentiation of rhabdomyosarcoma cells. *Oncogene* (e-pub ahead of print 25 February 2013; doi:10.1038/onc.2013.46).
31 Ciarapica R, Russo G, Verginelli F, Raimondi L, Donfrancesco A, Rota R *et al.* Deregulated expression of miR-26a and Ezh2 in rhabdomyosarcoma. *Cell Cycle* 2009; **8**: 172–175.
32 Marchesi I, Fiorentino FP, Rizzolio F, Giordano A, Bagella L. The ablation of EZH2 uncovers its crucial role in rhabdomyosarcoma formation. *Cell Cycle* 2012; **11**: 3828–3836.
33 Mai A, Valente S, Cheng D, Perrone A, Ragno R, Simeoni S *et al.* Synthesis and biological validation of novel synthetic histone/protein methyltransferase inhibitors. *ChemMedChem* 2007; **2**: 987–991.
34 Valente S, Lepore I, Dell'Aversana C, Tardugno M, Castellano S, Sbardella G *et al.* Identification of PR-SET7 and EZH2 selective inhibitors inducing cell death in human leukemia U937 cells. *Biochimie* 2012; **94**: 2308–2313.
35 Wong CF, Tellam RL. MicroRNA-26a targets the histone methyltransferase enhancer of zeste homolog 2 during myogenesis. *J Biol Chem* 2008; **283**: 9836–9843.
36 Juan AH, Kumar RM, Marx JG, Young RA, Sartorelli V. Mir-214-dependent regulation of the polycomb protein Ezh2 in skeletal muscle and embryonic stem cells. *Mol Cell* 2009; **36**: 61–74.
37 Shen X, Kim W, Fujiwara Y, Simon MD, Liu Y, Mysliwiec MR *et al.* Jumonji modulates polycomb activity and self-renewal versus differentiation of stem cells. *Cell* 2009; **139**: 1303–1314.
38 Peng JC, Valouev A, Swigut T, Zhang J, Zhao Y, Sidow A *et al.* Jarid2/Jumonji coordinates control of PRC2 enzymatic activity and target gene occupancy in pluripotent cells. *Cell* 2009; **139**: 1290–1302.
39 Valentijn LJ, Koster J, Haneveld F, Aissa RA, van Sluis P, Broekmans ME *et al.* Functional MYCN signature predicts outcome of neuroblastoma irrespective of MYCN amplification. *Proc Natl Acad Sci USA* 2012; **109**: 19190–19195.
40 Tan J, Yang X, Zhuang L, Jiang X, Chen W, Lee PL *et al.* Pharmacologic disruption of Polycomb-repressive complex 2-mediated gene repression selectively induces apoptosis in cancer cells. *Genes Dev* 2007; **21**: 1050–1063.
41 Palacios D, Mozzetta C, Consalvi S, Caretti G, Saccone V, Proserpio V *et al.* TNF/p38alpha/polycomb signaling to Pax7 locus in satellite cells links inflammation to the epigenetic control of muscle regeneration. *Cell Stem Cell* 2010; **7**: 455–469.
42 Miranda TB, Cortez CC, Yoo CB, Liang G, Abe M, Kelly TK *et al.* DZNep is a global histone methylation inhibitor that reactivates developmental genes not silenced by DNA methylation. *Mol Cancer Ther* 2009; **8**: 1579–1588.
43 Gannon OM, Merida de Long L, Endo-Munoz L, Hazar-Rethinam M, Saunders NA. Dysregulation of the repressive H3K27 trimethylation mark in head and neck squamous cell carcinoma contributes to dysregulated squamous differentiation. *Clin Cancer Res* 2012; **19**: 428–441.

44 Benoit YD, Laursen KB, Witherspoon MS, Lipkin SM, Gudas LJ. Inhibition of PRC2 histone methyltransferase activity increases TRAIL-mediated apoptosis sensitivity in human colon cancer cells. *J cell physiol* 2012; **228**: 764–772.
45 Cheng LL, Itahana Y, Lei ZD, Chia NY, Wu Y, Yu Y *et al.* TP53 genomic status regulates sensitivity of gastric cancer cells to the histone methylation inhibitor 3-deazaneplanocin A (DZNep). *Clin Cancer Res* 2012; **18**: 4201–4212.
46 Wachtel M, Dettling M, Koscielniak E, Stegmaier S, Treuner J, Simon-Klingenstein K *et al.* Gene expression signatures identify rhabdomyosarcoma subtypes and detect a novel t(2;2)(q35;p23) translocation fusing PAX3 to NCOA1. *Cancer Res* 2004; **64**: 5539–5545.
47 Davicioni E, Anderson MJ, Finckenstein FG, Lynch JC, Qualman SJ, Shimada H *et al.* Molecular classification of rhabdomyosarcoma--genotypic and phenotypic determinants of diagnosis: a report from the Children's Oncology Group. *Am J Pathol* 2009; **174**: 550–564.
48 Ren YX, Finckenstein FG, Abdueva DA, Shahbazian V, Chung B, Weinberg KI *et al.* Mouse mesenchymal stem cells expressing PAX-FKHR form alveolar rhabdomyosarcomas by cooperating with secondary mutations. *Cancer Res* 2008; **68**: 6587–6597.
49 Gomes MD, Lecker SH, Jagoe RT, Navon A, Goldberg AL. Atrogin-1,a muscle-specific F-box protein highly expressed during muscle atrophy. *Proc Natl Acad Sci USA* 2001; **98**: 14440–14445.
50 Sandri M, Sandri C, Gilbert A, Skurk C, Calabria E, Picard A *et al.* Foxo transcription factors induce the atrophy-related ubiquitin ligase atrogin-1 and cause skeletal muscle atrophy. *Cell* 2004; **117**: 399–412.
51 Cao L, Yu Y, Bilke S, Walker RL, Mayeenuddin LH, Azorsa DO *et al.* Genome-wide identification of PAX3-FKHR binding sites in rhabdomyosarcoma reveals candidate target genes important for development and cancer. *Cancer Res* 2010; **70**: 6497–6508.
52 Jiang Y, Singh P, Yin H, Zhou YX, Gui Y, Wang DZ *et al.* Opposite roles of myocardin and atrogin-1 in L6 myoblast differentiation. *J cell physiol* 2013; **228**: 1989–1995.
53 Ogata T, Machida S, Oishi Y, Higuchi M, Muraoka I. Differential cell death regulation between adult-unloaded and aged rat soleus muscle. *Mech ageing Dev* 2009; **130**: 328–336.
54 Fernando P, Kelly JF, Balazsi K, Slack RS, Megeney LA. Caspase 3 activity is required for skeletal muscle differentiation. *Proc Natl Acad Sci USA* 2002; **99**: 11025–11030.
55 Hunt LC, Upadhyay A, Jazayeri JA, Tudor EM, White JD. Caspase-3, myogenic transcription factors and cell cycle inhibitors are regulated by leukemia inhibitory factor to mediate inhibition of myogenic differentiation. *Skelet muscle* 2011; **1**: 17.
56 Moresi V, Williams AH, Meadows E, Flynn JM, Potthoff MJ, McAnally J *et al.* Myogenin and class II HDACs control neurogenic muscle atrophy by inducing E3 ubiquitin ligases. *Cell* 2010; **143**: 35–45.
57 Tintignac LA, Lagirand J, Batonnet S, Sirri V, Leibovitch MP, Leibovitch SA. Degradation of MyoD mediated by the SCF (MAFbx) ubiquitin ligase. *J biol chem* 2005; **280**: 2847–2856.
58 Okada A, Ono Y, Nagatomi R, Kishimoto KN, Itoi E. Decreased muscle atrophy F-box (MAFbx) expression in regenerating muscle after muscle-damaging exercise. *Muscle Nerve* 2008; **38**: 1246–1253.
59 Lagirand-Cantaloube J, Cornille K, Csibi A, Batonnet-Pichon S, Leibovitch MP, Leibovitch SA. Inhibition of atrogin-1/MAFbx mediated MyoD proteolysis prevents skeletal muscle atrophy *in vivo*. *PLoS One* 2009; **4**: e4973.
60 Xie P, Guo S, Fan Y, Zhang H, Gu D, Li H. Atrogin-1/MAFbx enhances simulated ischemia/reperfusion-induced apoptosis in cardiomyocytes through degradation of MAPK phosphatase-1 and sustained JNK activation. *J biol chem* 2009; **284**: 5488–5496.
61 Davicioni E, Anderson JR, Buckley JD, Meyer WH, Triche TJ. Gene expression profiling for survival prediction in pediatric rhabdomyosarcomas: a report from the children's oncology group. *J Clin Oncol* 2010; **28**: 1240–1246.
62 Kikuchi K, Tsuchiya K, Otabe O, Gotoh T, Tamura S, Katsumi Y *et al.* Effects of PAX3-FKHR on malignant phenotypes in alveolar rhabdomyosarcoma. *Biochem Biophys Res Commun* 2008; **365**: 568–574.
63 Ramirez-Peinado S, Alcazar-Limones F, Lagares-Tena L, El Mjiyad N, Caro-Maldonado A, Tirado OM *et al.* 2-deoxyglucose induces Noxa-dependent apoptosis in alveolar rhabdomyosarcoma. *Cancer Res* 2011; **71**: 6796–6806.
64 Crose LE, Etheridge KT, Chen C, Belyea B, Talbot LJ, Bentley RC *et al.* FGFR4 blockade exerts distinct antitumorigenic effects in human embryonal versus alveolar rhabdomyosarcoma. *Clin Cancer Res* 2012; **18**: 3780–3790.
65 Lee MH, Jothi M, Gudkov AV, Mal AK. Histone methyltransferase KMT1A restrains entry of alveolar rhabdomyosarcoma cells into a myogenic differentiated state. *Cancer Res* 2011; **71**: 3921–3931.
66 Momparler RL, Idaghdour Y, Marquez VE, Momparler LF. Synergistic antileukemic action of a combination of inhibitors of DNA methylation and histone methylation. *Leuk Res* 2012; **36**: 1049–1054.
67 Boumber Y, Issa JP. Epigenetics in cancer: what's the future? *Oncology* 2012; **25**: 220–226228.
68 Lawlor ER, Thiele CJ. Epigenetic changes in pediatric solid tumors: promising new targets. *Clin Cancer Res* 2012; **18**: 2768–2779.
69 Fan T, Jiang S, Chung N, Alikhan A, Ni C, Lee CC *et al.* EZH2-dependent suppression of a cellular senescence phenotype in melanoma cells by inhibition of p21/CDKN1A expression. *Mol Cancer Res* 2011; **9**: 418–429.
70 Chng KR, Chang CW, Tan SK, Yang C, Hong SZ, Sng NY *et al.* A transcriptional repressor co-regulatory network governing androgen response in prostate cancers. *Embo J* 2012; **31**: 2810–2823.
71 Simone C, Forcales SV, Hill DA, Imbalzano AN, Latella L, Puri PL. p38 pathway targets SWI-SNF chromatin-remodeling complex to muscle-specific loci. *Nat genet* 2004; **36**: 738–743.
72 Bray M, Driscoll J, Huggins JW. Treatment of lethal Ebola virus infection in mice with a single dose of an S-adenosyl-L-homocysteine hydrolase inhibitor. *Antiviral Res* 2000; **45**: 135–147.
73 Vekony H, Raaphorst FM, Otte AP, van Lohuizen M, Leemans CR, van der Waal I *et al.* High expression of Polycomb group protein EZH2 predicts poor survival in salivary gland adenoid cystic carcinoma. *J Clin Pathol* 2008; **61**: 744–749.

Supplementary Information accompanies this paper on the Oncogene website (http://www.nature.com/onc)